Scientia Pharmaceutica

ÖSTERREICHISCHE PHARMAZEUTISCHE GESELLSCHAFT

MDPI

Article

Improved Solubility and Dissolution Rates in Novel Multicomponent Crystals of Piperine with Succinic Acid

Erizal Zaini [1,*], Afriyani Afriyani [1], Lili Fitriani [1], Friardi Ismed [2], Ayano Horikawa [3] and Hidehiro Uekusa [3]

[1] Department of Pharmaceutics, Faculty of Pharmacy, Andalas University, Padang 25163, Indonesia; afriyani_sky@yahoo.co.id (A.); lilifitriani@phar.unand.ac.id (L.F.)
[2] Laboratory of Biota Sumatera and Faculty of Pharmacy, Andalas University, Padang 25163, Indonesia; friardi@phar.unand.ac.id
[3] Department of Chemistry, School of Science, Tokyo Institute of Technology, Tokyo 1528551, Japan; a.horikawa.chem@gmail.com (A.H.), uekusa@chem.titech.ac.jp (H.U.)
* Correspondence: erizal@phar.unand.ac.id

Received: 18 March 2020; Accepted: 9 April 2020; Published: 13 April 2020

Abstract: The objectives of this study were to prepare and characterize a novel piperine–succinic acid multicomponent crystal phase and to evaluate the improvement in the solubility and dissolution rate of piperine when prepared in the multicomponent crystal formation. The solid-state characterization of the novel multicomponent crystal was performed by powder X-ray diffraction (XRD), differential scanning calorimetry (DSC), and Fourier transform-infrared (FT-IR) spectroscopy. Solubility and dissolution rate profiles were evaluated in distilled water. The physical stability was evaluated under high relative humidity (75% and 100% RH). The determination of the single crystal X-ray diffraction structure revealed that this novel multicomponent crystal was a cocrystalline phase of piperine–succinic acid (2:1 molar ratio). The differential scanning calorimetry thermogram of the cocrystal showed a single and sharp endothermic peak at 110.49°C. The cocrystal resulted in greater solubility and a faster dissolution rate of piperine than intact piperine. This improvement was a result of the formation of a channel structure in the cocrystal. In addition, the cocrystal was stable under a humid condition.

Keywords: piperine; multicomponent crystal; cocrystal; succinic acid; dissolution rate

1. Introduction

Piperine is a major secondary metabolite isolated from plants of the *Piperaceae* family, especially from *Piper nigrum* L., which is known as the king of spices. These species are cultivated in tropical regions, such as Indonesia, Brazil, and India [1,2]. This plant has been widely used as both a household spice and a traditional medicine [3]. Ethnopharmacologically, pepper has been used to relieve pain and inflammation, and to improve gastrointestinal functionality [4–6]. Many studies have showed that piperine has diverse and valuable pharmacological activities, such as analgesic, anti-inflammatory, antibacterial, antidiabetic, and antioxidant effects [7–11]. In addition, piperine has been used to improve cognitive function and as a protective agent against neural degeneration and memory impairment [12]. Furthermore, piperine has been used as a bioenhancer when coadministered with some active pharmaceutical ingredients, such as rapamycin, curcumin, domperidone, and anti-tuberculosis drugs [13–16]. Unfortunately, the pharmaceutical application of piperine is limited by its low solubility in aqueous medium. Poorly water-soluble drugs have low bioavailability; dissolution is the rate-limiting step in the absorption process in the gastrointestinal

tract fluid. Nearly 70 to 80 % drugs currently in development have low solubility in water [17]. A major challenge faced by pharmaceutical manufacturers is the successful formulation of solid dosage forms that have a low solubility and dissolution rate of the active pharmaceutical ingredients. The bioavailability of active pharmaceutical ingredients in systemic circulation was significantly influenced by the solubility and dissolution rate properties in aqueous medium. The solubility was notably affected by the properties of its solid form, such as a crystalline form, amorphization, hydrophobicity, and surface area [18]. To optimize the physicochemical properties of active pharmaceutical ingredients, it is important to explore a proper solid form in order to launch a successful drug formulation [19].

Efforts to improve the solubility and dissolution rates of piperine have been investigated, including the development of a solid dispersion system with several polymers and water-soluble carriers [20,21], the formation of inclusion complexes with cyclodextrin [22–24], and the reduction of the particle size to nanoscale [25–27]. Although these methods have improved the solubility of piperine, some problems remain. The solid dispersions with polymers may be hygroscopic [28]. In addition, polymers and cyclodextrins have high molecular weights and low miscibility with active pharmaceutical ingredients; thus, the final dose of the complex with polymers and cyclodextrins is also high. The inclusion complex formation with cyclodextrin also faces some challenges when a drug is not able to form a strong interaction within the cavity, resulting in insignificant solubility improvement [29]. Moreover, the problem of the physical stability of the active pharmaceutical ingredient (API) during the manufacturing process and storage is still a challenge. The amorphous state tends to recrystallize to a more stable form, which will impact the variability of the dissolution rate of the API in the solid dosage form. The crystalline phase is preferred in dosage forms to overcome phase transitions during processing and storage [30,31].

To date, a popular strategy to alter physicochemical properties, such as solubility and dissolution rate, is the formation of a multicomponent crystal phase. A multicomponent crystal with a small organic molecule is likely to have high stability owing to its crystalline state. The final dose is also small due to the low molecular weight of the coformer. Thus, multicomponent crystals with small organic molecules offer significant advantages over other complex formations. Therefore, in this study, we focused on the formation of the multicomponent crystals of piperine. In general, a multicomponent crystal phase includes a salt, cocrystal, hydrate, and solvate [32,33]. Numerous studies have demonstrated that the formation of a multicomponent crystal phase of API with a suitable excipient could enhance its physicochemical properties, such as solubility and dissolution rate, permeability, bioavailability, physical stability, compressibility, and pharmacological efficacy [34–39]. To the best of our knowledge, only two studies on the multicomponent crystal phase of piperine have been reported: a cocrystal with resveratrol, and a salt with a halide [40,41]. The cocrystal of resveratrol and piperine was investigated to improve the solubility of resveratrol, and thus, a solubility study of piperine was not conducted. Although the crystal structure of the [Piperine(H)][I_3] salt was reported, its solubility was not studied. Therefore, there has not been a study on solubility improvement obtained with the multicomponent crystals. Piperine has three crystal forms (form I, II, and III). These crystal forms show remarkable differences in their physicochemical properties, such as melting point and solubility. Form I is the most stable polymorph and has a lower intrinsic dissolution rate than forms II and III; the melting point of form I is 131.38 °C [42].

In the current study, we prepared a novel cocrystal of piperine with a generally recognized as safe (GRAS) excipient as per FDA methods. It is notable that piperine does not form an inorganic salt with commonly used reagents such as HCl or HBr (Kennedy et al., 2018); hence, we selected an organic acid as the coformer. The piperine molecule does not have any functional groups with which to form a salt with organic acids. Thus, for a multicomponent crystal of piperine, cocrystal formation with organic acids is required. When piperine forms a cocrystal with resveratrol, the oxygen atom of the ketone of piperine acts as a hydrogen bond acceptor and forms hydrogen bonds with water and the hydroxyl group of resveratrol. Thus, piperine is expected to form a cocrystal with a molecule that has a hydrogen bond donor group. Succinic acid was selected as the coformer to form the cocrystal;

this process should improve the solubility and dissolution rates of piperine. Succinic acid, classified as a GRAS excipient by the FDA, forms cocrystals with many active pharmaceutical ingredients. In addition, succinic is a dicarboxylic acid with two hydrogen bond donor groups (COOH). After coformer screening, the cocrystal of piperine–succininic acid (2:1 molar ratio) was prepared by the slurry technique. The physicochemical properties of the cocrystal phase were investigated by powder X-ray diffraction analysis, differential scanning calorimetry (DSC) thermal analysis, Fourier transform-infrared (FT-IR) spectroscopy, and a solubility test in aqueous medium. The crystal structure of the new cocrystalline phase was confirmed by single crystal X-ray diffraction analysis. The dissolution profile of the piperine–succinic acid cocrystal was determined using a type II United States Pharmacopeia (USP) dissolution test apparatus.

2. Materials and Methods

2.1. Materials

Piperine was purchased from Tokyo Chemical Industry (TCI) Tokyo, Japan. Succinic acid was purchased from Merck, Germany. Ethanol and ethyl acetate were obtained from Merck, Germany. All other solvents used in this research were of analytical grade.

2.2. Methods

2.2.1. Preparation of Cocrystals of Piperine–Succinic Acid

The cocrystals of piperine–succinic acid (2:1 molar ratio) were prepared by the slurry method. Firstly, piperine (0.078 g; 0.000273 mol) and succinic acid (0.0170 g; 0.000143 mol) were weighed accurately and placed in a mortar. Then, 0.4 ml of ethanol was added and the mixture was ground manually by using a pestle until the solvent evaporated; this process was repeated, and the resultant sample was referred to as the liquid-assisted grinding (LAG) sample. In a sealed glass container, piperine (0.4491 g; 0.00157 mol) and succinic acid (0.0929 g; 0.00078 mol) were mixed with ethyl acetate. The LAG sample (0.0125 g) was added into the glass container and stirred for more than 24 hours by using a magnetic stirrer, which is known as the slurry method. The cocrystals obtained were filtered and stored in a desiccator.

2.2.2. Characterization of Cocrystal Piperine–Succinic Acid

2.2.2.1. Powder X-ray Diffraction Analysis

Powder X-ray diffraction (PXRD) analysis was performed at room temperature by using a Panalytical PW 30/40 X-ray diffractometer (The Netherlands). The diffractogram was recorded from $2\theta = 5°$ to 40°. The X-ray diffractometer was programmed as follows: target metal, Cu; filter, Kα; voltage, 45 kV; and current, 40 mA.

2.2.2.2. Single Crystal X-Ray Diffraction Analysis

The piperine–succinic acid single crystal for single crystal X-ray diffraction was prepared by solvent coevaporation from ethanol. Single-crystal X-ray diffraction data were collected in ω-scan mode by using an R-AXIS RAPID II diffractometer (Rigaku) with a CuKα radiation (λ = 1.54186 Å) rotating-anode source with VariMax007 optics. The integrated and scaled data were empirically corrected for absorption effects using ABSCOR. The initial structures were solved using direct methods with SHELXT, and then refined with SHELXL. All nonhydrogen atoms were refined anisotropically. All hydrogen atoms were found in a different Fourier map; however, they were placed by geometrical calculations and treated by a riding model during the refinement.

2.2.2.3. Differential Scanning Calorimetry

The thermodynamic properties of piperine, succinic acid, and the cocrystal were measured using a DSC apparatus (SETARAM Type EVO-131, Lyon, France), which was calibrated using indium. Approximately 5 mg of each sample was placed in an aluminum pan, and the temperature was increased from 50 °C to 250 °C at a rate of 10 °C/min.

2.2.2.4. Fourier Transform-Infrared Spectroscopy Analysis

Intermolecular interactions were studied using a FT-IR spectrophotometer (Perkin Elmer FT-IR, USA). The sample was mixed with dry potassium bromide in a weight ratio of 1:100, and this mixture was compressed into pellets. The absorption of samples was recorded between 4000 cm^{-1} and 600 cm^{-1}. The analysis was performed for intact piperine, intact succinic acid, and the cocrystal.

2.2.2.5. Solubility Test

The saturated solubility in CO_2-free distilled water was evaluated at room temperature using an orbital shaker. An excess amount of sample was added to 100 ml medium, equilibrated for 24 h, and then filtered through a membrane filter. The concentration of piperine was determined from the absorbance measurement at 341 nm by using an ultraviolet-visible light (UV-Vis) spectrophotometer (Genesys 10S Spectrophotometer, Madison, WI, USA).

2.2.2.6. In Vitro Dissolution Rate Profiles

The in vitro dissolution profiles of intact piperine, cocrystal, and physical mixture were determined using a type II United States Pharmacopeia (USP) dissolution testing apparatus (Hanson Research SR08PLUS, USA). The physical mixture at the same ratio as that of the cocrystal was prepared as comparison for dissolution rate profile study. Prior to the dissolution test, all samples were sieved in a range of 150–250 µm particle size. The equipment was adjusted to a speed of 50 rpm in 900 ml dissolution medium (CO_2-free distilled water). The temperature was maintained at 37 °C ± 0.5 °C. At predetermined times (5, 10, 15, 30, 45, and 60 min), an aliquot of approximately 5 mL was collected and filtered through filter paper. The concentration of piperine dissolved in the medium was determined by from the absorbance measurement at a maximum wavelength of 341 nm using a UV-vis spectrophotometer (Genesys 10S Spectrophotometer, USA). The experiment was conducted in triplicate. The data are presented as a chart (time vs. percentage of dissolved piperine).

2.2.2.7. Stability Test

Cocrystal samples which were prepared by the slurry method as described in 2.2 were tested for their stability. The samples were placed at 40 °C in each humidity (75% and 100%) for one week. The 75% RH condition was prepared with a saturated aqueous solution of NaCl.

2.2.2.8. Hydration Energy Calculation

The hydration energy was calculated using Spartan'16 V1.0.0 as described in the previous study [43] under the conditions of SM54, B3LYP_D3, and 6-311+G**. For this calculation, API and coformer neutral molecules used had been optimized for structure under the same software and conditions.

3. Results and Discussion

PXRD analysis is an important technique for the determination of solid-state properties such as crystalline phase, amorphization, and solid-state reaction behavior. Multicomponent crystals (cocrystal or salt) between two solid phases are confirmed when the PXRD pattern of the solid shows a unique pattern that differs from its starting materials. The PXRD patterns of piperine, succinic acid, and the cocrystal of piperine–succinic acid (2:1 molar ratio) are displayed in Figure 1. The diffraction pattern of intact piperine showed distinct and sharp diffraction peaks at 2θ values of 14.91°, 19.68°, 22.50°, 25.85°, and 28.25°, indicating a solid form with a highly crystalline nature. This PXRD pattern indicated that the piperine crystal was of form I. Furthermore, the intact succinic acid demonstrated

characteristic diffraction peaks at 2θ values of 16.09°, 18.98°, 20.06°, 26.17°, 31.53°, 32.52°, 38.09°, and 38.42°. The diffraction pattern of the cocrystal showed a unique pattern with 2θ values of 8.56°, 9.92°, 12.40°, 13.98°, 20.91°, 24.53°, 28.01°, and 29.21°, which corresponded to the formation of a new multicomponent crystal phase. In general, the multicomponent crystal phase can either be salt-type or cocrystal-type. In the salt-type multicomponent crystal, proton transfers occur between the active pharmaceutical ingredients and the coformer. Meanwhile, in the cocrystal, proton transfers cannot occur [44]. This characterization can be confirmed by single crystal XRD structure determination.

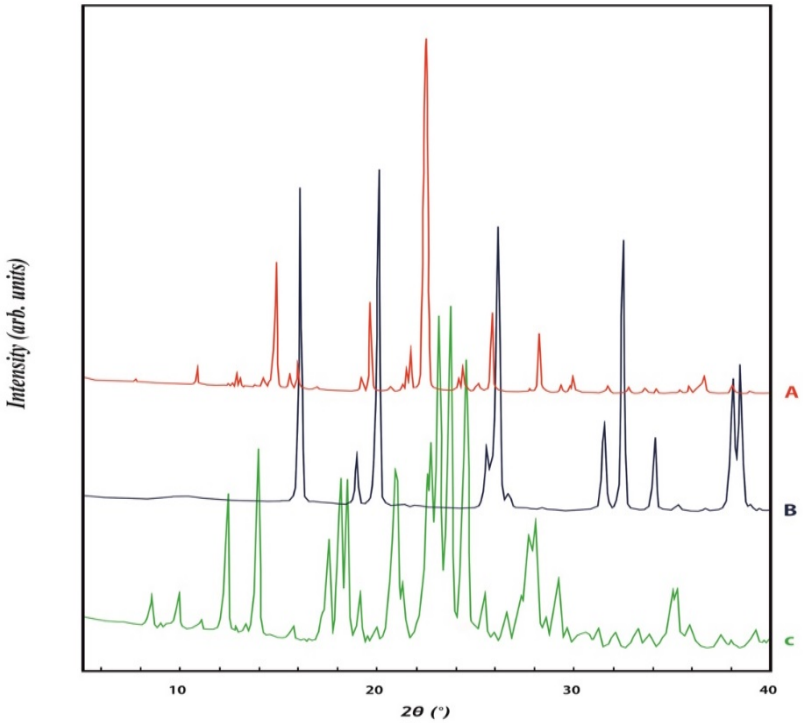

Figure 1. The powder X-ray diffraction pattern of (A) piperine, (B) succinic acid, and (C) the cocrystal of piperine–succinic acid (2:1 molar ratio).

DSC analysis is a rapid and simple method to screen for the formation of the multicomponent crystal phase between two solid materials [45,46]. The DSC thermogram of the intact piperine, intact succinic acid, and multicomponent crystal is depicted in Figure 2. The sharp endothermic peak at 131.38 °C indicates the melting point of piperine. This form is the most stable form I, and was similar to a previous report [42]. In addition, intact succinic acid showed an endothermic peak at 191.33 °C, which was attributed to its melting point. The DSC thermogram of the cocrystal of piperine–succinic acid exhibited a single sharp endothermic peak at 110.49 °C. This new peak was the melting point of the multicomponent crystal of piperine and succinic acid. Notably, the melting point of the piperine–succinic acid multicomponent crystal was lower than that of the parent API and its coformer. Thermodynamically, the melting point properties of the crystalline phase represent the intermolecular bonding in the crystal structure and lattice energy, and may affect the solubility and dissolution rate of crystalline solids in water [35,47].

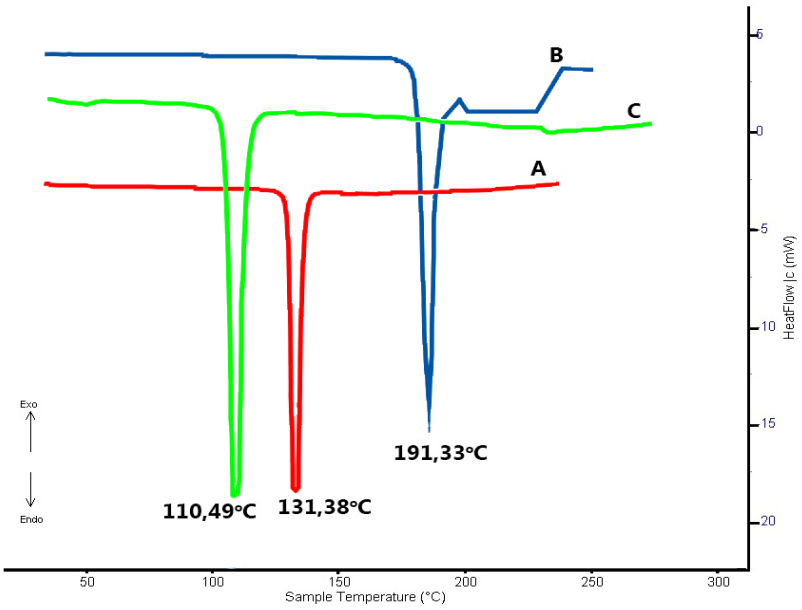

Figure 2. Differential scanning calorimetry thermogram of (A) piperine, (B) succinic acid, and (C) the cocrystal of piperine–succinic acid (2:1 molar ratio).

FT-IR spectroscopy analysis is a preliminary method used to determine the solid-state interaction between active pharmaceutical ingredients and excipients. The formation of multicomponent crystals indicates a significant difference in the molecular functional group vibrations compared with those of the individual components, based on supramolecular hetero- and homo-synthons [48]. The FT-IR spectra of intact piperine, intact succinic acid, and the cocrystal are displayed in Figure 3. The FTIR spectrum of intact succinic acid shows various characteristic peaks: OH stretching at 2919 cm^{-1} and 2634 cm^{-1}, carbonyl (C=O) stretching at 1678 cm^{-1}, and C–O–H bending vibration at 1410 cm^{-1} [49]. The FTIR analysis also shows the characteristic peaks of piperine, including aromatic C-H stretching at 3010 cm^{-1} and aliphatic C-H stretching at 2928 cm^{-1}, a carbonyl group (CO–N) at 1854 cm^{-1}, and aromatic (C=C) stretching at 1585 cm^{-1}. Furthermore, peaks at 1433 cm^{-1} were assigned to CH_2 bending and 1237 cm^{-1} to =C–O–C asymmetric stretching [50]. The FTIR spectrum of the cocrystal revealed several specific peaks. The peaks at 2936 cm^{-1} and 2600 cm^{-1} indicated O–H stretching from the hydrogen bond between a hydrogen of succinic acid and the ketone oxygen of piperine, based on the reported cocrystals of succinic acid with carbamazepine and itraconazole [51,52]. The other peaks were at 1818 cm^{-1} (1854 cm^{-1} for pure piperine), 1720 cm^{-1}, 1612 cm^{-1} (1678 cm^{-1} for pure succinic acid), and 1562 cm^{-1} (1584 cm^{-1} for pure piperine).

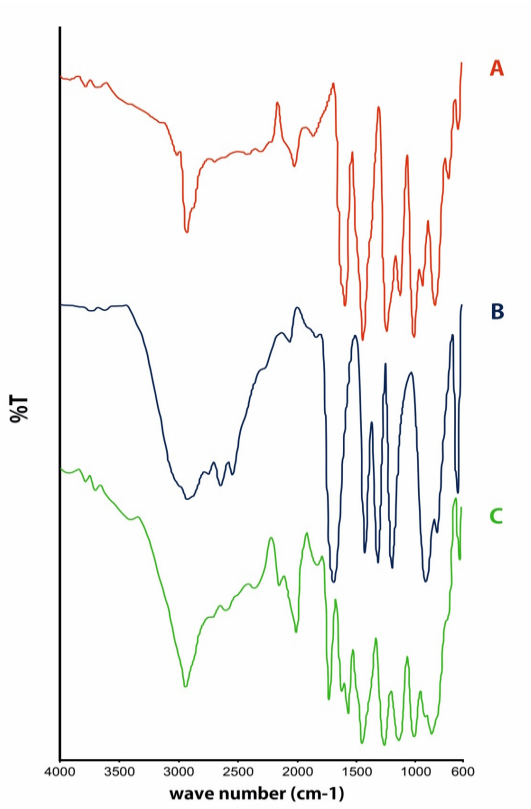

Figure 3. Fourier transform-infrared spectra of (A) piperine, (B) succinic acid, and (C) the cocrystal of piperine–succinic acid (2:1 molar ratio).

The single crystal structure analysis revealed the structure of piperine–succinic acid cocrystal. This specimen crystal was obtained from the EtOH solution by the evaporation method. The crystal data are shown in Table 1. The crystal system was monoclinic, and the space group was $P2_1/c$. The crystal structure showed that the ratio of piperine to succinic acid was 2:1. As the succinic acid molecule is at the center of symmetry, the asymmetric unit comprised one piperine molecule and half of the succinic acid molecule. As expected, the ketone oxygen atom of piperine and the carboxyl oxygen atom of succinic formed hydrogen bonds; thus, a piperine molecule was present on each side of succinic acid, as shown in Figure 4. The geometry of the carboxylic group is a good indicator of cocrystal or salt formation. The C=O and C–OH distances of succinic acid were 1.210(2) Å and 1.335(2) Å, respectively, indicating that the group was in a neutral form. In addition, significant residual electron density was observed for the H atom position in the COOH group during the crystal structure analysis. Therefore, this crystal was a cocrystal and not a salt crystal. Moreover, other hydrogen bonds were not observed. In the crystal structure, two piperine and one succinic acid molecules were connected by the OH...O hydrogen bonds to form a group of three molecules. This unit stacked to form a characteristic channel motif, as displayed in Figure 5. This packing consists of the self-stacking of the piperine part and the channel structure of succinic acid. This type of structure contributes to the solubility and dissolution rate improvement.

Table 1. Crystal data for the piperine–succinic acid cocrystal.

Parameter	Piperine–Succinic Acid
Moiety formula	$C_{17}H_{19}NO_3$, 0.5($C_4H_6O_4$)
Crystal system	Monoclinic
Space group	$P2_1/c$
a (Å)	4.1459(1)
b (Å)	9.6960(3)
c (Å)	41.1214(10)

ß(°)	92.703(2)
V (Å^3)	1651.19(8)
Z / *Z*′	4/1
T (K)	93
R-factor (%)	8.64

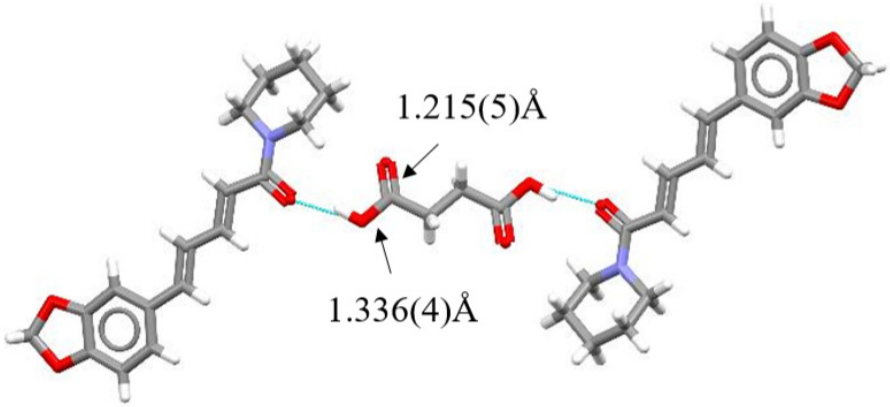

Figure 4. H-bond between piperine and succinic acid and the three-molecule unit of piperine and succinic acid.

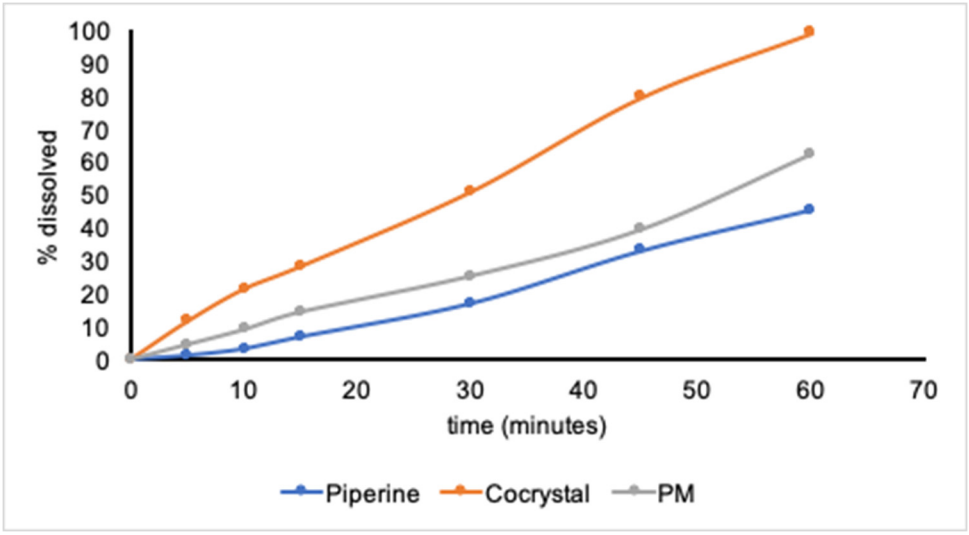

Figure 5. Dissolution rate profile of piperine (blue), physical mixture (grey), and the cocrystal (orange).

In the current study, we reported the novel cocrystal of piperine–succinic acid (2:1 molar ratio), which improved the solubility and dissolution rate, as shown in Table 2 and Figure 6. The solubility of the cocrystal increased approximately 4-fold compared with that of intact piperine. Consequently, the dissolution rate of the cocrystal also improved significantly. According to the Noyes–Whitney equation, the dissolution rate of the solid is proportional to its solubility [53]. Furthermore, the cocrystal of piperine–succinic acid showed a faster dissolution rate than that of intact piperine. The percentage of piperine dissolved from the cocrystal significantly improved compared to that of intact piperine and its physical mixture. In 60 min, 99.00% of piperine dissolved from the cocrystal, whereas only 45.30 and 62.22 % of intact piperine and physical mixture dissolved, respectively. The dissolution rate of the physical mixture of piperine–succinic acid increased slightly compared to

intact Piperine. This was due to the microenvironmental solubilizing effect of succinic acid which improves the wettability of piperine in aqueous medium [54,55].

Table 2. Solubility data for piperine and piperine–succinic acid in distilled water.

Compound	Solubility (μg/mL)	± SD
Piperine	2.93	± 0.04
Piperine–succinic acid	11.71	± 0.26

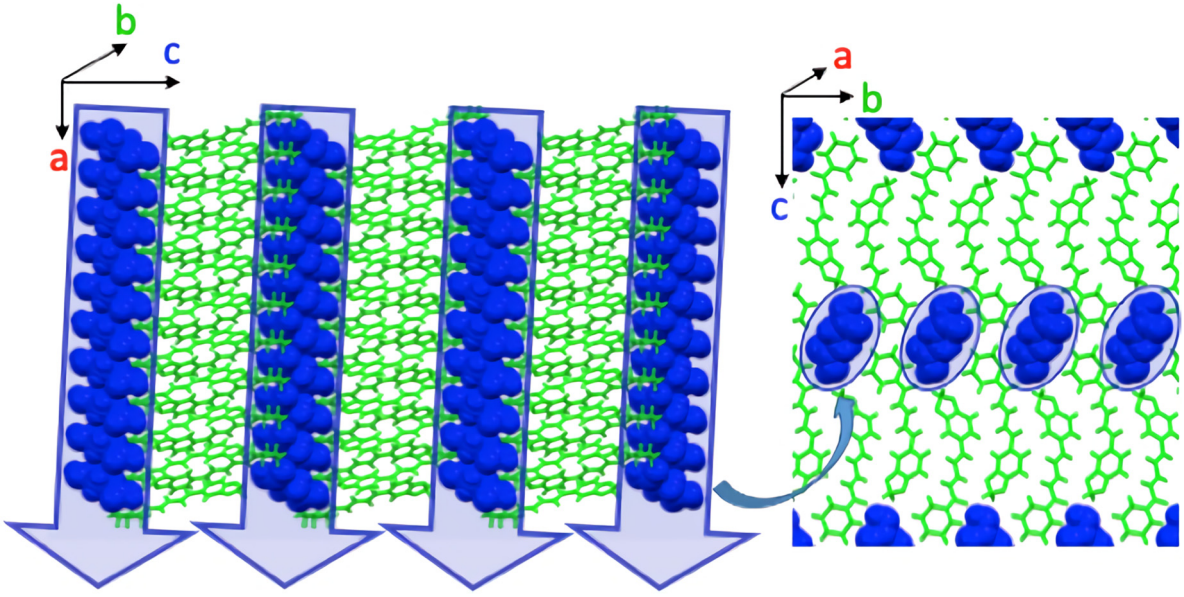

Figure 6. Channel motif of the succinic acid cocrystal (green, piperine; blue, succinic acid) with a-, b-, c-axis mark.

Several mechanisms are involved in the enhancement of the solubility and dissolution rate in the multicomponent crystal phase; changes in thermodynamic properties of the solid phase (melting point) may affect the solubility properties of the solid crystal. The melting point is correlated with the lattice energy of the crystal. A lower melting point indicates a weaker lattice energy in the crystalline phase, conferring greater solubility and a higher dissolution rate [34,47]. As described earlier, in the piperine–succinic acid cocrystal, succinic acid molecules formed a channel structure. Solubility enhancements arising from a channel structure have been reported previously, and this piperine–succinic acid cocrystal structure strongly indicated the occurrence of this improvement mechanism [56,57]. Putra et al. explained the mechanism as follows [58]: First, the more highly soluble coformer molecules dissolve from a cocrystal, leaving void channel structure in the crystal. As strong inter molecular interaction between the API and the conformer disappears, it makes the stability of the cocrystal lower. Thus, the remaining stacked API structure with only weaker inter molecular interactions would easily break up. This leads to the dissolution of API molecules, and an improvement in the solubility of the active pharmaceutical ingredient. In this study, the strong inter molecular interaction was the hydrogen bonds between piperine and succinic acid in the cocrystal; the succinic acid coformer formed the channel structure. Thus, this solubility improvement mechanism can be applied to the succinic acid cocrystal. A hydration energy calculation confirmed that the succinic acid molecule is calculated as more stabilized in water media than the piperine molecule. The hydration energies of these molecules are piperine: −34.62 kJ/mol and succinic acid: –53.68 kJ/mol. Together with the channel structure of succinic acid molecules, the solubility improvement mechanism of this cocrystal can also be explained by the same mechanism described above.

Furthermore, the stability of the succinic acid cocrystal with respect to humidity was confirmed. PXRD measurement revealed that the succinic acid cocrystals left for one week under high humidity

conditions (75% RH / 100% RH) were stable. Moreover, the PXRD of the tested samples showed no change during the test as seen in Figure 7.

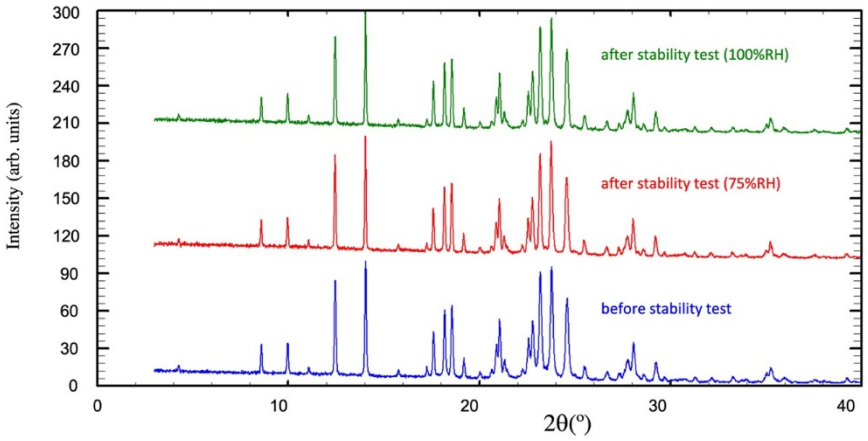

Figure 7. PXRD of piperine–succinic acid cocrystal before and after the stability test.

4. Conclusions

In this study, we successfully improved the solubility of piperine, an important constituent of black pepper, by rational formation of a cocrystal with succinic acid, a GRAS coformer. This was achieved despite the relatively poor propensity of the piperine molecule in forming hydrogen bonds. The solubility improvement mechanism was explained by the presence of a channel in the crystal structure. Although the cocrystal has higher solubility, it was stable under a humid condition. In addition, important properties of the cocrystal, measured by the DSC and FT-IR spectra, were presented to support the cocrystal formation. Our findings on the solubility improvement of poor hydrogen bond-forming compounds have provided an insight into methods to improve the physicochemical properties of similar compounds by cocrystal formation.

Author Contributions: Conceptualization, E.Z.; methodology, E.Z., A., L.F., H.U.; software, E.Z., H.U.,A.H.; validation, E.Z., H.U.; formal Analysis, E.Z., L.F., F.I., H.U.; investigation, L.F., A. A.H., resources, E.Z., F.I., L.F., H.U.; data curation, E.Z., A., L.F., H.U., A.H.; writing—original draft preparation, E.Z.; writing—review and editing, E.Z., L.F., H.U.; visualization, E.Z., L.F., A.H., H.U.; supervision, E.Z., F.I., L.F., H.U.; project administration, E.Z.; funding acquisition, E.Z., H.U.

Funding: This research was funded by Andalas University for Grant Research PGB contract number 25/UN.16.17/PP.PGB/LPPM/2018, JSPS KAKENHI Grant Number JP17K05745 and JP18H04504 for support.

Conflicts of Interest: The authors declare no conflict of interest.

References

1. Gorgani, L.; Mohammadi, M.; Najafpour, G.D.; Nikzad, M. Piperine—The Bioactive Compound of Black Pepper: From Isolation to Medicinal Formulations. *Compr. Rev. Food Sci. Food Saf.* **2017**, *16*, 124–40.
2. Damanhouri, Z.A. A Review on Therapeutic Potential of Piper nigrum L. (Black Pepper): The King of Spices. *Med. Aromat. Plants* **2014**, *3*, doi:10.4172/2167-0412.1000161.
3. Johri, R.K.; Zutshi, U. An Ayurvedic formulation "Trikatu" and its constituents. *J. Ethnopharmacol.* **1992**, *37*, 85–91.
4. Tasleem, F.; Azhar, I.; Ali, S.N.; Perveen, S.; Mahmood, Z.A. Analgesic and anti-inflammatory activities of Piper nigrum L. *Asian Pac. J. Trop. Med.* **2014**, *7*, S461–S468.
5. Meghwal, M.; Goswami, T.K. Piper nigrum and piperine: An update. *Phyther. Res.* **2013**, *27*, 1121–1130.
6. Butt, M.S.; Pasha, I.; Sultan, M.T.; Randhawa, M.A.; Saeed, F.; Ahmed, W. Black Pepper and Health Claims: A Comprehensive Treatise. *Crit. Rev. Food Sci. Nutr.* **2013**, *53*, 875–886.
7. Kharbanda, C.; Alam, M.S.; Hamid, H.; Javed, K.; Bano, S.; Ali, Y.; Dhulap, A.; Alam, P.; Pasha, M.A.Q. Novel Piperine Derivatives with Antidiabetic Effect as PPAR-γ Agonists. *Chem. Biol. Drug Des.* **2016**, *88*, 354–362.

8. Toyoda, T.; Shi, L.; Takasu, S.; Cho, Y.-M.; Kiriyama, Y.; Nishikawa, A.; Ogawa, K.; Tatematsu, M.; Tsukamoto, T. Anti-Inflammatory Effects of Capsaicin and Piperine on Helicobacter pylori-Induced Chronic Gastritis in Mongolian Gerbils. *Helicobacter* **2016**, *21*, 131–142.
9. Zarai, Z.; Boujelbene, E.; Ben Salem, N.; Gargouri, Y.; Sayari, A. Antioxidant and antimicrobial activities of various solvent extracts, piperine and piperic acid from Piper nigrum. *LWT Food Sci. Technol.* **2013**, *50*, 634–641.
10. Bukhari, I.A.; Alhumayyd, M.S.; Mahesar, A.L.; Gilani, A.H. The analgesic and anticonvulsant effects of piperine in mice. *J. Physiol. Pharmacol.* **2013**, *64*, 789.
11. Vijayakumar, R.S.; Surya, D.; Nalini, N. Antioxidant efficacy of black pepper (Piper nigrum L.) and piperine in rats with high fat diet induced oxidative stress. *Redox Rep.* **2004**, *9*, 105–110.
12. Wattanathorn, J.; Chonpathompikunlert, P.; Muchimapura, S.; Priprem, A.; Tankamnerdthai, O. Piperine, the potential functional food for mood and cognitive disorders. *Food Chem. Toxicol.* **2008**, *46*, 3106–3110.
13. Katiyar, S.S.; Muntimadugu, E.; Rafeeqi, T.A.; Domb, A.J.; Khan, W. Co-delivery of rapamycin- and piperine-loaded polymeric nanoparticles for breast cancer treatment. *Drug Deliv.* **2016**, *23*, 2608–2616.
14. Singh, S.; Kumar, P. Neuroprotective potential of curcumin in combination with piperine against 6-hydroxy dopamine induced motor deficit and neurochemical alterations in rats. *Inflammopharmacology* **2017**, *25*, 69–79.
15. Athukuri, B.L.; Neerati, P. Enhanced oral bioavailability of domperidone with piperine in male wistar rats: Involvement of CYP3A1 and P-gp inhibition. *J. Pharm. Pharm. Sci.* **2017**, *20*, 28–37.
16. Hegeto, L.A.; Caleffi-Ferracioli, K.R.; Nakamura-Vasconcelos, S.S.; de Almeida, A.L.; Baldin, V.P.; Nakamura, C.V.; Siqueira, V.L.D.; Scodro, R.B.L.; Cardoso, R.F. In vitro combinatory activity of piperine and anti-tuberculosis drugs in Mycobacterium tuberculosis. *Tuberculosis* **2018**, *111*, 35–40.
17. Lipinski, C.A. Drug-like properties and the causes of poor solubility and poor permeability. *J. Pharmacol. Toxicol. Methods* **2000**, *44*, 235–249.
18. Kawabata, Y.; Wada, K.; Nakatani, M.; Yamada, S.; Onoue, S. Formulation design for poorly water-soluble drugs based on biopharmaceutics classification system: Basic approaches and practical applications. *Int. J. Pharm.* **2011**, *420*, 1–10.
19. Blagden, N.; de Matas, M.; Gavan, P.T.; York, P. Crystal engineering of active pharmaceutical ingredients to improve solubility and dissolution rates. *Adv. Drug Deliv. Rev.* **2007**, *59*, 617–630.
20. Thenmozhi, K.; Yoo, Y.J. Enhanced solubility of piperine using hydrophilic carrier-based potent solid dispersion systems. *Drug Dev. Ind. Pharm.* **2017**, *43*, 1501–1509.
21. Ashour, E.A.; Majumdar, S.; Alsheteli, A.; Alshehri, S.; Alsulays, B.; Feng, X.; Gryczke, A.; Kolter, K.; Langley, N.; Repka, M.A. Hot melt extrusion as an approach to improve solubility, permeability and oral absorption of a psychoactive natural product, piperine. *J. Pharm. Pharmacol.* **2016**, *68*, 989–998.
22. Quilaqueo, M.; Millao, S.; Luzardo-Ocampo, I.; Campos-Vega, R.; Acevedo, F.; Shene, C.; Rubilar, M. Inclusion of piperine in β-cyclodextrin complexes improves their bioaccessibility and in vitro antioxidant capacity. *Food Hydrocoll.* **2019**, *91*, 143–152.
23. Suzuki, R.; Kanamoto, I.; Ezawa, T.; Tunvichien, S.; Inoue, Y. Changes in the Physicochemical Properties of Piperine/ β -Cyclodextrin due to the Formation of Inclusion Complexes. *Int. J. Med. Chem.* **2016**, *2016*, 1–9.
24. Ezawa, T.; Inoue, Y.; Murata, I.; Takao, K.; Sugita, Y.; Kanamoto, I. Characterization of the Dissolution Behavior of Piperine/Cyclodextrins Inclusion Complexes. *AAPS PharmSciTech* **2018**, *19*, 923–933.
25. Yusuf, M.; Khan, M.; Khan, R.A.; Ahmed, B. Preparation, characterization, in vivo and biochemical evaluation of brain targeted Piperine solid lipid nanoparticles in an experimentally induced Alzheimer's disease model. *J. Drug Target.* **2013**, *21*, 300–311.
26. Zafar, F.; Jahan, N.; Rahman, K.-U.; Bhatti, H.N. Increased Oral Bioavailability of Piperine from an Optimized Piper nigrum Nanosuspension. *Planta Med.* **2019**, *85*, 249–257.
27. Sedeky, A.S.; Khalil, I.A.; Hefnawy, A.; El-Sherbiny, I.M. Development of core-shell nanocarrier system for augmenting piperine cytotoxic activity against human brain cancer cell line. *Eur. J. Pharm. Sci.* **2018**, *118*, 103–112.
28. Rumondor, A.C.F.; Taylor, L.S. Effect of polymer hygroscopicity on the phase behavior of amorphous solid dispersions in the presence of moisture. *Mol. Pharm.* **2010**, *7*, 477–490.
29. Moyano, J.R.; Arias-Blanco, M.J.; Gines, J.M.; Rabasco, A.M.; Pérez-Martínez, J.I.; Mor, M.; Giordano, F. Nuclear Magnetic Resonance Investigations of the Inclusion Complexation of Gliclazide with β-Cyclodextrin. *J. Pharm. Sci.* **1997**, *86*, 72–75.
30. Konno, H.; Taylor, L.S. Ability of different polymers to inhibit the crystallization of amorphous felodipine in the presence of moisture. *Pharm. Res.* **2008**, *25*, 969–978.

31. Fitriani, L.; Haqi, A.; Zaini, E. Preparation and characterization of solid dispersion freeze-dried efavirenz—Polyvinylpyrrolidone K-30. *J. Adv. Pharm. Technol. Res.* **2016**, *7*, 105–109.
32. Vioglio, P.C.; Chierotti, M.R.; Gobetto, R. Pharmaceutical aspects of salt and cocrystal forms of APIs and characterization challenges. *Adv. Drug Deliv. Rev.* **2017**, *117*, 86–110.
33. Da Silva, C.C.; Guimarães, F.F.; Ribeiro, L.; Martins, F.T. Salt or cocrystal of salt? Probing the nature of multicomponent crystal forms with infrared spectroscopy. *Spectrochim. Acta Part A Mol. Biomol. Spectrosc.* **2016**, *167*, 89–95.
34. Zaini, E.; Fitriani, L.; Sari, R.Y.; Rosaini, H.; Horikawa, A.; Uekusa, H. Multicomponent Crystal of Mefenamic Acid and N-Methyl-D-Glucamine: Crystal Structures and Dissolution Study. *J. Pharm. Sci.* **2019**, *108*, 2341–2348.
35. Putra, O.D.; Umeda, D.; Nugraha, Y.P.; Nango, K.; Yonemochi, E.; Uekusa, H. Simultaneous Improvement of Epalrestat Photostability and Solubility via Cocrystallization: A Case Study. *Cryst. Growth Des.* **2018**, *18*, 373–379.
36. Machado, T.C.; Gelain, A.B.; Rosa, J.; Cardoso, S.G.; Caon, T. Cocrystallization as a novel approach to enhance the transdermal administration of meloxicam. *Eur. J. Pharm. Sci.* **2018**, *123*, 184–190.
37. Ainurofiq, A.; Mauludin, R.; Mudhakir, D.; Umeda, D.; Soewandhi, S.N.; Putra, O.D.; Yonemochi, E. Improving mechanical properties of desloratadine via multicomponent crystal formation. *Eur. J. Pharm. Sci.* **2018**, *111*, 65–72.
38. Yuliandra, Y.; Zaini, E.; Syofyan, S.; Pratiwi, W.; Putri, L.N.; Pratiwi, Y.S.; Arifin, H. Cocrystal of ibuprofen–nicotinamide: Solid-state characterization and in vivo analgesic activity evaluation. *Sci. Pharm.* **2018**, *86*, 23.
39. Serrano, D.R.; Walsh, D.; O'Connell, P.; Mugheirbi, N.A.; Worku, Z.A.; Bolas-Fernandez, F.; Galiana, C.; Dea-Ayuela, M.A.; Healy, A.M. Optimising the in vitro and in vivo performance of oral cocrystal formulations via spray coating. *Eur. J. Pharm. Biopharm.* **2018**, *124*, 13–27.
40. Kennedy, A.R.; King, N.L.C.; Oswald, I.D.H.; Rollo, D.G.; Spiteri, R.; Walls, A. Structural study of salt forms of amides; paracetamol, benzamide and piperine. *J. Mol. Struct.* **2018**, *1154*, 196–203.
41. He, H.; Zhang, Q.; Wang, J.R.; Mei, X. Structure, physicochemical properties and pharmacokinetics of resveratrol and piperine cocrystals. *CrystEngComm* **2017**, *19*, 6154–6163.
42. Pfund, L.Y.; Chamberlin, B.L.; Matzger, A.J. The bioenhancer piperine is at least trimorphic. *Cryst. Growth Des.* **2015**, *15*, 2047–2051.
43. Shao, Y.; Molnar, L.F.; Jung, Y.; Kussmann, J.; Ochsenfeld, C.; Brown, S.T.; Gilbert, A.T.B.; Slipchenko, L.V.; Levchenko, S.V.; O'Neill, D.P.; et al. Advances in methods and algorithms in a modern quantum chemistry program package. *Phys. Chem. Chem. Phys.* **2006**, *8*, 3172–3191.
44. Grothe, E.; Meekes, H.; Vlieg, E.; Ter Horst, J.H.; De Gelder, R. Solvates, Salts, and Cocrystals: A Proposal for a Feasible Classification System. *Cryst. Growth Des.* **2016**, *16*, 3237–3243.
45. Yamashita, H.; Hirakura, Y.; Yuda, M.; Teramura, T.; Terada, K. Detection of cocrystal formation based on binary phase diagrams using thermal analysis. *Pharm. Res.* **2013**, *30*, 70–80.
46. Lu, E.; Rodríguez-Hornedo, N.; Suryanarayanan, R. A rapid thermal method for cocrystal screening. *CrystEngComm* **2008**, *10*, 665.
47. Putra, O.D.; Yonemochi, E.; Uekusa, H. Isostructural Multicomponent Gliclazide Crystals with Improved Solubility. *Cryst. Growth Des.* **2016**, *16*, 6568–6573.
48. Saha, S.; Desiraju, G.R. Acid···Amide Supramolecular Synthon in Cocrystals: From Spectroscopic Detection to Property Engineering. *J. Am. Chem. Soc.* **2018**, *140*, 6361–6373.
49. Krishnan, S.; Raj, C.J.; Priya, S.M.N.; Robert, R.; Dinakaran, S.; Das, S.J. Optical and dielectric studies on succinic acid single crystals. *Cryst. Res. Technol.* **2008**, *43*, 845–850.
50. Dahiya, S.; Rani, R.; Dhingra, D.; Kumar, S.; Dilbaghi, N. Conjugation of epigallocatechin gallate and piperine into a zein nanocarrier: Implication on antioxidant and anticancer potential. *Adv. Nat. Sci. Nanosci. Nanotechnol.* **2018**, *9*, doi:10.1088/2043-6254/aad5c1.
51. Fuliaş, A.; Vlase, G.; Vlase, T.; Şuta, L.-M.; Şoica, C.; Ledeţi, I. Screening and characterization of cocrystal formation between carbamazepine and succinic acid. *J. Therm. Anal. Calorim.* **2015**, *121*, 1081–1086.
52. Ober, C.A.; Montgomery, S.E.; Gupta, R.B. Formation of itraconazole/L-malic acid cocrystals by gas antisolvent cocrystallization. *Powder Technol.* **2013**, *236*, 122–131.
53. Dokoumetzidis, A.; Macheras, P. A century of dissolution research: From Noyes and Whitney to the Biopharmaceutics Classification System. *Int. J. Pharm.* **2006**, *321*, 1–11.

54. Chiou, W.L.; Niazi, S. Pharmaceutical applications of solid dispersion systems: Dissolution of griseofulvin–succinic acid eutectic mixture. *J. Pharm. Sci.* **1976**, *65*, 1212–1214.
55. Ansari, M.T.; Pervez, H.; Shehzad, M.T.; Saeed-Ul-Hassan, S.; Mehmood, Z.; Shah, S.N.H.; Razi, M.T.; Murtaza, G. Improved physicochemical characteristics of artemisinin using succinic acid. *Acta Pol. Pharm. Drug Res.* **2014**, *71*, 451–462.
56. Furuta, H.; Mori, S.; Yoshihashi, Y.; Yonemochi, E.; Uekusa, H.; Sugano, K.; Terada, K. Physicochemical and crystal structure analysis of pranlukast pseudo-polymorphs II: Solvate and cocrystal. *J. Pharm. Biomed. Anal.* **2015**, *111*, 44–50.
57. Putra, O.D.; Furuishi, T.; Yonemochi, E.; Terada, K.; Uekusa, H. Drug-Drug Multicomponent Crystals as an Effective Technique to Overcome Weaknesses in Parent Drugs. *Cryst. Growth Des.* **2016**, *16*, 3577–3581.
58. Putra, O.D.; Umeda, D.; Nugraha, Y.P.; Furuishi, T.; Nagase, H.; Fukuzawa, K.; Uekusa, H.; Yonemochi, E. Solubility improvement of epalrestat by layered structure formation: Via cocrystallization. *CrystEngComm* **2017**, *19*, 2614–2622.